BNL-209670-2018-JAAM

Determination of Hydrogen Oxidation Reaction Mechanism Based on Pt-H-ad Energetics in Alkaline Electrolyte

J. Hu, K. Sasaki

To be published in "JOURNAL OF THE ELECTROCHEMICAL SOCIETY"

November 2018

Chemistry Department

Brookhaven National Laboratory

U.S. Department of Energy

USDOE Office of Science (SC), Basic Energy Sciences (BES) (SC-22)

Notice: This manuscript has been authored by employees of Brookhaven Science Associates, LLC under Contract No. DE-SC0012704 with the U.S. Department of Energy. The publisher by accepting the manuscript for publication acknowledges that the United States Government retains a non-exclusive, paid-up, irrevocable, world-wide license to publish or reproduce the published form of this manuscript, or allow others to do so, for United States Government purposes.

DISCLAIMER

This report was prepared as an account of work sponsored by an agency of the United States Government. Neither the United States Government nor any agency thereof, nor any of their employees, nor any of their contractors, subcontractors, or their employees, makes any warranty, express or implied, or assumes any legal liability or responsibility for the accuracy, completeness, or any third party's use or the results of such use of any information, apparatus, product, or process disclosed, or represents that its use would not infringe privately owned rights. Reference herein to any specific commercial product, process, or service by trade name, trademark, manufacturer, or otherwise, does not necessarily constitute or imply its endorsement, recommendation, or favoring by the United States Government or any agency thereof or its contractors or subcontractors. The views and opinions of authors expressed herein do not necessarily state or reflect those of the United States Government or any agency thereof.

Determination of Hydrogen Oxidation Reaction Mechanism Based on Pt—H_{ad} Energetics in Alkaline Electrolyte

Jue Hu [a,b], Kurian A. Kuttiyiel [b], Kotaro Sasaki [b*], Chengxu Zhang [a*], Radoslav R. Adzic [b*]

[a] Kunming University of Science and Technology, Kunming 650500, People's Republic of China

[b] Chemistry Department, Brookhaven National Laboratory, Upton, NY 11973, USA

Abstract

The understanding of the sluggish hydrogen oxidation reaction (HOR) kinetics in alkaline electrolyte is crucial for designing high performance electrocatalysts. Here, we report a clear and convincing result on this problem by investigating the relationship between the HOR kinetics and Pt-adsorbate energetics. Using electrochemical analysis for well-modified Pt surfaces with distinct Pt-adsorbate interactions, we establish a clear trend in activity for HOR in alkaline electrolyte, that is, the activity changes in the order Au@Pt < Pt < Pd@Pt < Ru@Pt. A decisive role of Pt—H_{ad} energetics in the HOR kinetics on Pt surfaces is determined, while no favorable effects of Pt—OH_{ad} energetics in the HOR kinetics were found. The nature of strong Pt—H_{ad} interaction for Pt/C catalyst in alkaline electrolyte is revealed by *in-situ* X-ray absorption near-edge structure (XANES) analysis. These insights play an important role for better understanding the mechanism and structure sensitivity for Pt catalyzed hydrogen oxidation/evolution reactions.

Key words: HOR, mechanism, Pt—H_{ad} energetics, alkaline electrolyte, well-modified Pt surfaces

1. Introduction

As the concerns about global warming, environmental pollution and energy security grow, the demand for using renewable energy sources instead of fossil fuel is expanding.[1-3] Hydrogen, which produces water as the only product during its oxidation reaction, is established as one of the most likely fuels of the future.[4] The "hydrogen-based economy" relies on the development of an efficient, durable and low cost hydrogen-oxygen fuel cell, a zero-emission device that can convert chemical energy of hydrogen directly into electricity.[5] Hydrogen oxidation reaction (HOR) as the key reaction in hydrogen-oxygen fuel cell has been widely investigated, and ultra low loading Pt ($\leqslant$0.05 mg cm^{-2}) is required for HOR in proton exchange membrane fuel cells.[6-7] However, the HOR and HER (hydrogen evolution reaction) kinetics becomes sluggish in base, which is at least two orders of magnitude slower than that in acid.[8] The sluggish HOR kinetics in alkaline electrolyte hinders the development of alkaline exchange membrane fuel cell, which is more commercially viable because of the potential to forego noble metal catalysts and less serious corrosion.[9] To obtain the catalysts with high HOR activity in alkaline environment, it is essential to understand the reason for this puzzling difference of HOR kinetics in acid and base. Significant progress has been made through the combination of experimental and theoretical studies to probe the reaction mechanisms both in acid and alkaline electrolytes.[3, 10-12]

The classic model states that the best catalyst for HOR should have optimal binding energy with adsorbed hydrogen (H_{ad}) whether in acidic or alkaline electrolytes.[5] Markovic and co-workers first reported an inspiring bifunctional HOR/HER mechanism in alkaline solution.[4] They demonstrated a decisive role of adsorbed hydroxyl species (OH_{ad}) in the HOR reaction on both the metallic surfaces (Ir and $Pt_{0.1}Ru_{0.9}$) and metal hydroxyl ($Ni(OH)_2$) decorated Pt surfaces, and suggested that the HOR is controlled by both the substrate-H_{ad} and substrate-OH_{ad} energetics.[4, 13-14] However, combining density functional calculations and voltammetric behavior of RuPt alloy, Zhuang and co-workers argued that the incorporation of Ru that posed an electronic effect can weaken the Pt—H_{ad} interaction, resulting in the enhancement of HOR activity of RuPt alloy.[15] Sheng and co-workers elucidated that the HOR activity in alkaline condition can be solely correlated with the hydrogen binding energy on monometallic surfaces *vis* a volcano type of relationship.[16] They studied HOR performance on Pt in buffer solutions at different pH, which further supported their conclusion that hydrogen binding energy can thus be considered as the sole reaction descriptor for HOR/HER kinetics.[17]

Although previous studies have helped to realize the decisive role of substrate-intermediate energetics in the HOR mechanism, key questions, viz. which interaction (substrate-H_{ad} or substrate-OH_{ad}) plays the key role to decide the HOR kinetics, and why the rate of the HOR is at least two orders of magnitude lower in base than in acid, remain unanswered. Electronic properties govern the binding energies between the catalyst atoms and adsorbates, so fine-tuning of the electronic properties of metal

surface can give us a way to control the metal-adsorbates interaction and thus help to understand the reaction mechanism. Therefore, in the present work, we firstly design four Pt surfaces with different electronic properties to evaluate the relationship between the HOR kinetics and Pt-adsorbates (Pt—H_{ad} or Pt—OH_{ad}) energetics: Ru@Pt with weak Pt-adsorbates (H_{ad} and OH_{ad}) interaction, Au@Pt with strong Pt-adsorbates interaction, Pd@Pt and Pt with intermediate Pt-adsorbates interaction.[18-19] To the best of our knowledge, no studies focusing on a systematic understanding of variations in the catalytic properties of HOR based on well-characterized Pt surfaces with different electronic structure have been established. We then investigate which Pt-adsorbates interaction plays the decisive role in the HOR kinetics on Pt surface, Pt—H_{ad} monotonic effect, or Pt—H_{ad} and Pt—OH_{ad} bifunctional effect

2. Experimental Section

2.1. Preparation of M@Pt core-shell nanoparticles

Synthesis of Ru@Pt/C nanoparticles.

The Ru@Pt/C core-shell nanoparticles were synthesized by the ethanol-based approach.[11] In a typical procedure, 80 ml anhydrous ethanol (200 proof, ACS/USP Grade, Pharmco Aaper) solution containing calculated amount of $RuCl_3$ (Sigma-Aldrich) was refluxed at 110 °C with rigorous stirring for 1 h, during which the color of the solution turned from brown to olive green. Meanwhile, vulcan XC72R carbon black was mixed with 60 ml anhydrous ethanol in an ultrasonic bath for 30 min. After then, the obtained carbon dispersion and 0.2 M NaOH aqueous solution were added into the $RuCl_3$ solution in sequence. The mixture was rigorously stirred for 2 h at 110 °C

to ensure a complete reaction. After cooling to room temperature, the resulted slurry was filtered, rinsed with ethanol and MilliQ water (18.2 MΩ, Millipore UV Plus) and dried in a vacuum oven at 50 °C overnight and subsequently annealed in H_2 at 450 °C for 1 h.

The as-synthesized Ru/C sample was first dispersed in 100 ml anhydrous ethanol by sonicating for 30 min, followed by refluxed at 110 °C for 1 h. After cooling to room temperature, calculated amount of H_2PtCl_6 (Sigma-Aldrich) ethanolic solution was dropped into the slurry. The mixture was rigorously stirred at 80 °C for 2-3 h until the solution became colorless. Then, the mixture was cooled down, filtered rinsed and vacuum dried. The Ru@Pt/C core-shell nanoparticles with a 1:1 Ru:Pt atomic ratio were prepared.

Synthesis of Pd@Pt/C nanoparticles.

The Pd@Pt/C core-shell nanoparticles can also be synthesized using the ethanol-based approach. Experimental details have been described in the previous paper [20]. In the typical procedure, Pd@Pt/C nanoparticles were synthesized by mixing a 1: 1 metal atomic ratio of commercial Pd/C (10 wt%, E-TEK) and H_2PtCl_6 with anhydrous ethanol under rigorous stirring, followed by heating to 80 °C for 2-3 h until the solution became colorless, and subsequent adding calculated amount of NaOH solution to ensure a complete reaction. After then, the mixture was filtered and rinsed with ethanol and MilliQ water, and vacuum dried. The Pd@Pt/C core-shell nanoparticles with a 1:1 Pd:Pt atomic ratio were prepared.

Synthesis of Au@Pt/C nanoparticles.

The Au@Pt/C core-shell nanoparticles were prepared using two steps: (1) synthesizing Au nanoparticle core by $NaBH_4$ reduction approach, and (2) synthesizing Pt shell by ethanol-based approach. In the typical synthesis of Au/C nanoparticles, 20 ml $NaBH_4$ (Sigma-Aldrich) aqueous solution (30 mM) was dropped into an 600 ml solution containing calculated amount of $HAuCl_4$ (Sigma-Aldrich) and 80 mg of sodium citrate. The mixture was stirred at room temperature for 30 min to ensure a complete reaction, and then heated to 40 °C for 30 min to remove the residual $NaBH_4$. Au nanoparticles were then loaded on the carbon surface by mixing the Au colloidal solution with an uniform dispersed vulcan XC72R carbon slurry. After vigorous stirring for 2 days at room temperature, the Au/C nanoparticles were obtained by filtering, rinsing and drying. Then, Au@Pt core-shell nanoparticles with a 1:1 Au:Pt atomic ratio were prepared by Pt coating the as-obtained Au/C nanoparticles using the same procedure described above.

Pt/C nanoparticles.

Commercial carbon supported Pt nanoparticles with the Pt loading of 46.6 wt% (Tanaka Kikinzoku International Inc.) were obtained, and used as received without further purification. The average Pt particle diameter is 2.6 nm.

2.2. Characterization

XAS measurements using an electrochemical cell were undertaken at the BL2-2 beamline at Stanford Synchrotron Radiation Lightsource (SSRL). The catalyst sample

(working electrode), an ion exchange membrane, and a Pt thin foil (counter electrode) were sandwiched and clamped tightly by the two acrylic plastic bodies. Each plastic body has an X-ray window. The electrolyte was 0.1 M KOH and an Ag/AgCl leak-free electrode was used as a reference electrode. Details of the electrochemical cell, which is a modified version of that described in literature,[21] are given elsewhere.[22] The data acquired by the electrochemical cell were processed and analyzed by Athena software.[23]

2.3. Electrochemical measurements

Electrochemical measurements were carried out in a three-electrode test cell by using a Volta PGZ402 potentiostat (Voltalab, Radiometer Analytical). The catalyst ink was prepared by ultrasonic mixing of 4 mg of the catalyst with 2 ml MilliQ water, 2 ml iso-propanol (Mallinck-Baker) and 8 µl 5wt% Nafion solution (perfluorinated resin, Aldrich) until a dark and uniform aqueous dispersion was obtained. A thin film of the catalyst was prepared on a glassy carbon rotating disk electrode (RDE) with the area of 0.196 cm^2 (5 mm diameter, Pine Research Instrumentation) by placing 10-20 µl of the obtained dispersion, and then dried in air at room temperature. The Pt loadings for the Pt/C, Ru@Pt/C, Pd@Pt/C and Au@Pt/C catalysts were 21.9, 19.0, 15.8 and 16.4 µg cm^{-2}, respectively. The RDE with catalyst was mounted onto a rotator (Pine Research Instrumentation) as the working electrode. A Pt foil was served as the counter electrode, and leak-free Hg/HgO (1M NaOH) electrode electrode was served as the reference electrode in alkaline electrolyte. The electrochemical measurements were all performed at room temperature, and the potential were referenced to that of the reversible

hydrogen electrode (RHE). All electrochemical measurements were carried out in alkaline electrolyte (0.1 M KOH). The HER-HOR measurements were performed in H_2-saturated electrolytes by averaging the polarization curve measured during cathodic and anodic sweeps at the scan rate of 10 mV s^{-1} and rotation rates of 400, 625, 900, 1025, 1600, 2025 and 2500 rpm. The resistance was determined by ac impedance spectra tested immediately after HER-HOR measurements and used for iR-correcting the measured polarization curves. Cyclic Voltammetry (CV) characterization was carried out in the potential rage from 0.05 to 1.1 V vs. RHE at a scan rate of 20 mV s^{-1} in a Ar-saturated electrolyte.

3. Results and Discussion

3.1. Evaluation the relationship between the HOR kinetics and Pt-adsorbates

The Ru@Pt/C, Pd@Pt/C and Au@Pt/C core-shell structure catalysts with two layers of Pt shell were synthesized step by step following the procedure of the ethanol-based approach.[11] Scanning transmission electron microscopy with a high-angle annular dark field (HAADF-STEM) combined with density functional theory (DFT) calculation verified the core-shell structure and thickness dependency of Pt shell on Pt percentage for the ethanol-synthesized metal@Pt catalysts in previous papers.[11, 20] The activity of catalyst toward the HOR and HER in alkaline media was evaluated in an H_2-saturated 0.1 M KOH solution. Typical polarization curves on Au@Pt/C, Pd@Pt/C and Ru@Pt/C core-shell structure catalysts and commercial Pt/C catalyst are shown in Figure 1a. All these curves are plotted against the ohmic loss corrected potential ($E_{\text{iR-free}}$). As shown in Figure 1a, the geometric current densities (mA cm^{-2} geo) for HER increases linearly

with the decrease in potential and the HER activity trend increases in the order of Ru@Pt/C > Pd@Pt/C > Pt/C > Au@Pt/C within the measured potential range. In the HOR region, the geometric current densities for all the catalysts increase along with the potential increase until they attain the limiting current density (i_{lim}) due to the limited H_2 mass transport. Figure 1b shows the i_{lim} normalized HOR polarization curves for four Pt surfaces on different metal core substrate. For comparison, Figure 1b also displays the i_{lim} normalized HOR diffusion current density (i_d) according to the Nernstian diffusion overpotential (η_{diff}) expression: [17, 24]

$$\eta_{diff} = -\frac{RT}{n_{HOR}F}\ln\left(1-\frac{i_d}{i_{lim}}\right) \quad (1)$$

where R, T and F corresponding to gas constant (8.314 J mol^{-1} K^{-1}), temperature (*e.g.*, 293K) and Faraday constant (96485 A s mol^{-1}), respectively. n_{HOR}=2, as two electrons are involved in the oxidation of one H_2 molecule. The i_{lim} normalized HOR polarization curve deviating from the Nernstian diffusion overpotential exhibits a slow HOR kinetics because the latter assumes infinitely fast reaction kinetics.[25] The HOR activity follows the order Ru@Pt/C > Pd@Pt/C > Pt/C > Au@Pt/C in alkaline solution under the same experimental conditions.

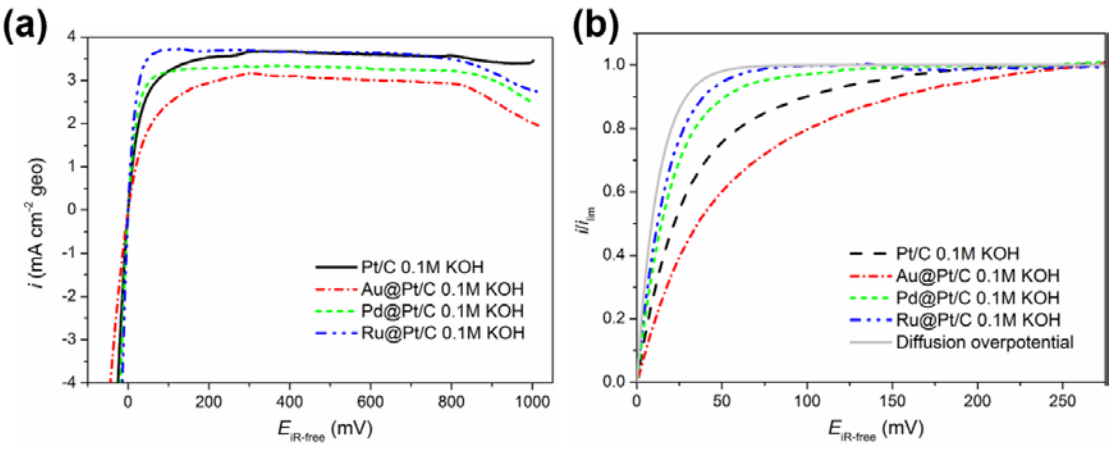

Figure 1. HOR activities on different Pt core-shell catalysts in alkaline solution. (a) Ohmic loss corrected HOR/HER polarization curves on Pt catalysts in a H_2-saturated 0.1 M KOH solution at 2500 rpm with a potential scan rate of 10 mV s^{-1}. Pt loading for Pt/C, Ru@Pt/C, Pd@Pt/C and Au@Pt/C catalysts were 21.9, 19.0, 15.8 and 16.4 μg cm^{-2}, respectively. (b) HOR polarization curves normalized to the limiting current density. The diffusion overpotential curve (grey line) is also shown in (b).

For the electrocatalysis reactions, the catalysts' activities depend sensitively on the energetics of the interactions between the metal surfaces and the key reaction intermediates, including adsorption, bond making, bond breaking and desorption.[26] The mechanism of the HOR on Pt surface is typically treated as a combination of two out of three elementary steps: Tafel-Volmer or Heyrovsky-Volmer, including the dissociative adsorption of H_2, dissociative ionization of H_2 and oxidative desorption of adsorbed H (H_{ad}).[27-28]

Tafel step (dissociative adsorption):

$$H_2 \rightarrow 2H_{ad} \qquad (2)$$

Heyrovsky step (dissociative ionization):

in acid: $$H_2 + H_2O \rightarrow H_{ad} + H_3O^+ + e^- \qquad (3a)$$

in base: $$H_2 + OH^- \rightarrow H_{ad} + H_2O + e^- \qquad (3b)$$

Volmer step: (oxidative desorption):

in acid: $$H_{ad} + H_2O \rightarrow H_3O^+ + e^- \qquad (4a)$$

in base: $$H_{ad} + OH^- \rightarrow H_2O + e^- \qquad (4b)$$

A plot of overpotential (η) *vs*. log(i_k), known as the Tafel plot, is a useful method for evaluating reaction kinetics. Kinetic current density (i_k) is extracted from the raw

polarization curves using the Koutecky-Levich equation.[8]

$$i_k = \frac{i \times i_{lim}}{i_{lim} - i} \quad (5)$$

Figure 2a displays iR-corrected potential-kinetic current density curves for HOR. For a quantitative comparison, the geometric current density was normalized by the Pt electrochemical surface area determined by CO-stripping (shown in Figure S1) to yield the specific kinetic current density (mA cm^{-2}).[29] As shown in Figure 2a, the Tafel plots recorded on Ru@Pt/C, Pd@Pt/C, Au@Pt/C and Pt/C catalysts exhibited classical Tafel behavior. After fitting the linear part at large overpotential of the Tafel plot, the Tafel slopes of Ru@Pt/C, Pd@Pt/C, Pt/C and Au@Pt/C catalysts were determined to be 34.2, 95.3, 117.4 and 129.0 mV dec^{-1}, respectively. The Tafel slope of the commercial Pt/C catalyst (117.4 mV dec^{-1}) agrees well with the values in the references.[25, 30] As expected, the systematic modification of Pt surface, with different metal core, exhibits a HOR activity trend (Figure 2b) for Ru@Pt/C > Pd@Pt/C > Pt/C > Au@Pt/C in alkaline solution.

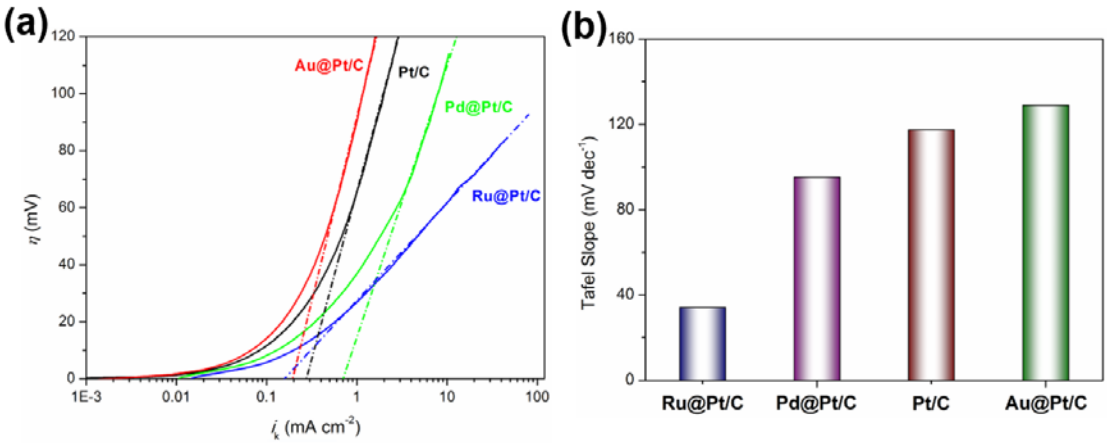

Figure 2. (a) HOR Tafel plots of the kinetic current densities on different Pt core-shell catalysts in 0.1 M KOH solution. (b) Trend in Tafel Slope for HOR as a function of the core metals.

Previous studies have unambiguously shown that the rate of HOR in both acid and alkaline media is determined by the rate limiting steps.[8, 31] As mentioned above, the Nernstian diffusion-controlled HOR is assumed as the infinitely fast reaction kinetics, which indicates that the dissociative reaction (Tafel or Heyrovsky step) and oxidative reaction (Volmer step) are so quick that the reaction rate is only determined by the rate of H_2 diffusion from the electrolyte to the catalysts' surface. Therefore, the Tafel slope for Nernstian diffusion-controlled HOR, as the lowest HOR Tafel slope, is $\approx$29 mV dec^{-1} at 293 K derived from the Butler-Volmer equation (see Supporting Information note 1 and Figure S2), which agrees well with the value ($\approx$30 mV dec^{-1}) in the literature.[32] According to the literature the Tafel slope value within the range from 30 to 40 mV dec^{-1} is attributed to the slow dissociative adsorption of H_2, we deduce that the charge transfer step (Heyrovsky or Volmer step) is very fast on the Ru@Pt surface.[30, 33] The high Tafel slopes of the Pd@Pt/C, Pt/C and Au@Pt/C catalysts indicate that the charge transfer step is the rate determining step on these three Pt surfaces.[8] Density functional theory (DFT) calculations showed that the binding energies between the catalyst atoms and adsorbates correlated well with the position of *d*-band center of catalyst.[34] The strongly compressive strain and electronic effects in the Ru@Pt core-shell structure catalyst induced lower-lying *d* states and *d*-band center down-shift of Pt atoms, resulting in the weakening of the Pt-adsorbate bonding.[18-19] The relatively weak interaction between the Pt atoms and H_{ad} at the Ru@Pt catalyst surface accelerates the H_{ad} desorption from the Pt surface, and as a result, the Tafel slope the HOR on the Ru@Pt surface is much smaller than that on pure Pt surface, and fast charge transfer

Heyrovsky or Volmer step on the Ru@Pt surface. On the contrary, because the Au lattice constant is larger than the Pt lattice constant, the tensile strain leads to up-shift of the d-band center of the Pt on Au@Pt catalyst surface.[19] The Au@Pt catalyst may suffer from hindered HOR kinetics owing to the stronger bonding of intermediates, and is therefore less active than pure Pt.

3.2. Which interaction plays the key role to decide the HOR kinetics, Pt—H_{ad} or Pt—OH_{ad}?

We use the linear part of the polarization curve within a micro-polarization region (-5 to +5 mV vs. RHE in this work) to obtain the exchange current density (i_0) from the linearized form of the Butler-Volmer equation (see Supporting Information note 2):[35]

$$i_0 = \frac{i_k RT}{\eta nF} = \frac{RT}{R_{ct} nF} \quad (6)$$

Figure S3 shows the magnification of kinetic current density in the vicinity of the reversible overpotential, which yields straight lines with the slope corresponding to the i_0. Charge transfer resistance (R_{ct}) can also be calculated from equation (6) as 60.5, 90.2, 129.7 and 155.4 Ω cm^2 for Ru@Pt/C, Pd@Pt/C, Pt/C and Au@Pt/C catalysts, respectively. The exchange current densities changes in the order Au@Pt/C (0.081 mA cm^{-2}) < Pt/C (0.097 mA cm^{-2}) < Pd@Pt/C (0.140 mA cm^{-2}) < Ru@Pt/C (0.209 mA cm^{-2}), which gives the trend of absolute kinetic activities of these four different Pt surfaces. This is an additional evidence, consistent with the Tafel slope results, that Pt-intermediate energetics serves as the key influential factor for HOR kinetics.

However, to determine which Pt-intermediate interactions (Pt—H_{ad} or Pt—OH_{ad}) is playing the key role to decide the HOR kinetics, we used cyclic voltammetry (CV) as

the fundamental method for characterizing electrochemical surfaces that has a direct link to the energetics of adsorption processes on metal surfaces.[36] Thus, using CVs we determined the surface coverage (θ) of chemisorbed hydrogen (H_{upd}) and hydroxyl species (OH_{ad}) from the hydrogen adsorption/desorption and OH adsorption/desorption regions respectively by dividing ECSAs calculated by CO stripping curves using the same method in the literatures.[3, 26] As shown in Figure 3a, the CV curves of these four different Pt surfaces contain the hydrogen adsorption/desorption (H_{upd}) region (below 0.35 V vs. RHE for Ru@Pt/C and below 0.45 V vs. RHE for Pt/C, Pd@Pt/C and Au@Pt/C catalysts), followed by a double-layer region, and subsequent OH adsorption/desorption (OH_{ad}) region (above 0.4 V vs. RHE for Ru@Pt/C and above 0.5 V vs. RHE for Pt/C, Pd@Pt/C and Au@Pt/C catalysts).[4, 15] Accordingly, the surface coverage of chemisorbed hydrogen (θ_{Hupd}) trend on different Pt surfaces is clearly observed in Figure 3b. The Ru@Pt catalyst which possesses the weakest Pt—H_{ad} interaction exhibits the lowest θ_{Hupd}. Pd@Pt and Pt show higher θ_{Hupd} owing to the stronger Pt—H_{ad} interaction. As for the Au@Pt catalyst, the strongest interaction between Pt atoms and H_{ad} leads to the highest coverage of H_{ad}. The charge corresponding to the hydrogen absorption/desorption is strongly dependent on the nature of the electronic structure of Pt surface, and they follow the order Ru@Pt < Pd@Pt < Pt < Au@Pt. The trend in the values of θ_{Hupd} as a function of the Pt electronic structure demonstrates that this quantity correlates well with the Pt—H_{ad} energetics. As such, this result is an excellent foundation to understand the kinetics of electrochemical reactions, if the rates of these reactions are controlled by the Pt—H_{ad} energetics.

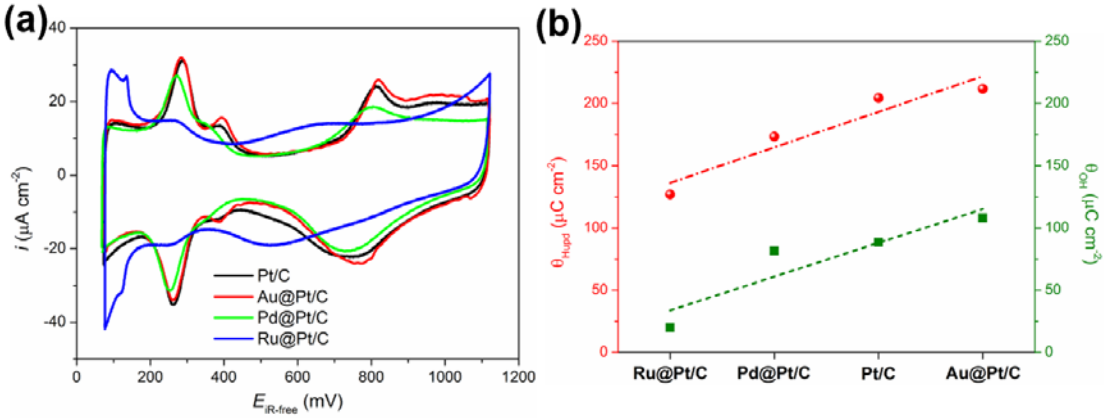

Figure 3. (a) Ohmic loss corrected voltammograms on Pt catalysts in an Ar-saturated 0.1 M KOH solution with a potential scan rate of 20 mV s^{-1}. (b) Comparison of H_{upd} and OH charges as a function of the core metals.

To evaluate the HOR kinetics, we summarize the HOR activities of these four Pt surfaces as a function of θ_{Hupd} in Figure 4a. Indeed, Figure 4 reveals that the HOR kinetics is inversely proportional to the Pt—H_{ad} bonding strength, that is, the activity increases with a linear relationship with θ_{Hupd} in the order of Au@Pt < Pt < Pd@Pt < Ru@Pt. In regard to the HOR mechanism, the splitting of one hydrogen molecule into two hydrogen ions must involve both the breaking of H–H bond and the dissociation of Pt—H_{ad}. Indeed, the HOR activity of catalysts strikes a balance between the cleaving of H–H bond and desorption of H_{ad}, and therefore generates a volcano-type dependence of catalytic activity on catalyst-H_{ad} bonding strength.[16] As has been demonstrated, a surface with lower-lying *d* states, like Pt surface supported on Ru core, tends to bond H_{ad} more weakly, thereby facilitating the desorption of H_{ad} but decreasing the kinetics of H–H bond breaking, suggesting Tafel step as the rate determining step. On the other hand, a surface with higher-lying *d* states, like Pt surface in Pd@Pt, Pt or Au@Pt catalysts, tends to bond H_{ad} more strongly, thereby hindering the Pt—H_{ad} dissociation,

suggesting that the HOR rate is limited by removal of adsorbed H_{ad} (Volmer step). These findings are in line with our predictions that the Pt—H_{ad} bonding strength plays a decisive role on the HOR kinetics. Having established the significance of the H_{ad} desorption on Pt surfaces with different Pt—H_{ad} bonding strengths, we turned to the effect of OH_{ad} interactions on Pt surface by determining the coverage of OH_{ad} based on the cyclic voltammetry (CV) results.[3, 26] It is clear from Figure 4b that the trend of OH_{ad} coverage on different Pt surfaces, which is in line with the results in literature, shows the same trend of Pt—H_{ad} bonding strength.[37] Ru@Pt catalyst which possesses the highest HOR activity has the weakest Pt—OH_{ad} bond, and on the contrary, Au@Pt catalyst which possesses the lowest HOR activity has the strongest Pt—OH_{ad} bond. Thus, it is hard to conclude a positive role of OH_{ad} in the HOR kinetics on the Pt surfaces under current conditions.

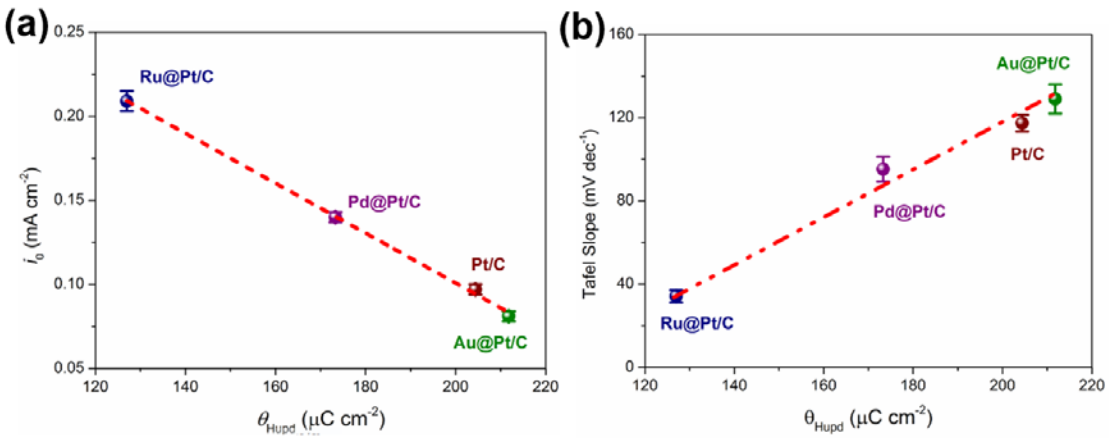

Figure 4. Trend in the (a) exchange current density and (b) Tafel slope for HOR in alkaline solution as a function of the H_{upd} charges. Error bars stand for the variation of at least two sets of experimental repeats.

3.3. Nature of the Pt—H_{ad} bonding for strong and weak Pt—H_{ad} energetics

We thus have established a decisive role of Pt—H_{ad} energetics on the HOR kinetics.

The trend in the values of HOR activity as a function of the H_{ad} coverage indicates that this quantity correlates well with the Pt—H_{ad} bonding. A long-standing problem in the research of H chemisorption on Pt catalysts is the ambiguity about the nature of the Pt—H_{ad} bonding for strongly and weakly bonded hydrogen. Further study the Pt—H_{ad} bonding difference between Pt/C and Ru@Pt/C catalysts is crucial for better understanding the reason of the sluggish HOR kinetics for Pt/C in alkaline electrolyte. Therefore, *in-situ* X-ray absorption spectra (XAS) on Ru@Pt/C and Pt/C nanoparticles in 0.1 M KOH solution, with and without chemisorbed hydrogen, were analyzed. There are obvious differences between Pt surfaces from the Pt/C nanoparticles and the Ru@Pt/C nanoparticles, both in the extended X-ray absorption fine structure (EXAFS) region (R-space) and in the X-ray absorption near-edge structure (XANES) region. Figure 5a depicts the Fourier transform (FT) magnitudes of EXAFS data (R-space) for Ru@Pt/C and Pt/C nanoparticles, and Pt foil. A slightly left-shift of the peak around 2.1 Å corresponding to the Pt—Pt bond of Ru@Pt/C nanoparticles compared to that of Pt/C nanoparticles and Pt foil may due to the compression effect of Pt shell on Ru core.[38] To elucidate the origin of the observed difference in Pt—H_{ad} energetics on pure Pt surface from the Pt surface with Ru core, we measured *in-situ* XANES spectra of Pt L_3 edge for Pt/C and Ru@Pt/C nanoparticle at different potentials, shown in Figure 5b and 5c and Figure S5. The $\Delta\mu_{H1}$, $\Delta\mu_{H2}$ and $\Delta\mu_{DL}$ are corresponding to the white line intensity at the potential of 0.05 V *vs.* RHE, 0.26 V *vs.* RHE and double-layer potential (0.45 V *vs.* RHE for Pt/C and 0.35 V *vs.* RHE for Ru@Pt/C in base were derived from the CV curves in Figure 4a), respectively. Pt in double-layer region is regarded as a clean

surface because the interactions between Pt and ions or H_2O are the smallest. It is clear that the intensity of the white line ($\Delta\mu$) decreased in the presence of H_{ad} (H_{upd} region) for both Pt/C and Ru@Pt/C nanoparticles. This phenomenon is attributed to the decrease in Pt *d*-band vacancies as a result of electronic interaction between Pt atoms and adsorbates.[39] The data offer strong evidence of a potential dependence of H_{ad} desorption from Pt surface. There is more evidence in the relative changes of Pt L_3 edge white line intensity $(\Delta\mu_x - \Delta\mu_y)/\Delta\mu_{DL}$ for Pt/C and Ru@Pt/C nanoparticles as a function of potential, as shown in Figure 5d. Since the Pt—H_{ad} bonding strength can be deduced from the electrochemical behavior,[15] three potential regions were chosen to study the Pt—H_{ad} energetics on these two different Pt surfaces, that is, lower potential range from 0.05 V *vs.* RHE to 0.26 V *vs.* RHE ($\Delta\mu_{H2} - \Delta\mu_{H1}$) as the region for the weaker H_{ad} desorption, higher potential range from 0.26 V *vs.* RHE to double-layer potential ($\Delta\mu_{DL} - \Delta\mu_{H2}$) as the region for the stronger H_{ad} desorption, and total H_{upd} potential range from 0.05 V to double-layer potential ($\Delta\mu_{DL} - \Delta\mu_{H1}$) as the region for the total adsorbed H desorption. The larger change of the intensity in the total H_{ad} desorption region ($\Delta\mu_{DL} - \Delta\mu_{H1}$) for Pt/C nanoparticle relative to Ru@Pt/C nanoparticles proved a higher H_{ad} coverage on the pure Pt surface than that on the Pt surface with Ru core, which is consistent with the electrochemical analysis. It is clear in Figure 5d that two types of H_{ad} (weakly bonded H and strongly bonded H) are bonded on Pt surface for both the Pt/C and Ru@Pt/C nanoparticles due to the different Pt—H_{ad} bonding strength. Further comparing the intensity changes of Pt/C and Ru@Pt/C nanoparticles in the weaker H_{ad} and stronger H_{ad} desorption regions, it is worth to notice that a higher total H_{ad} coverage

on pure Pt surface is mainly due to the higher coverage of strongly bonded H_{ad}. This is also the main reason leading to the much stronger Pt — H_{ad} energetics of Pt/C nanoparticles.

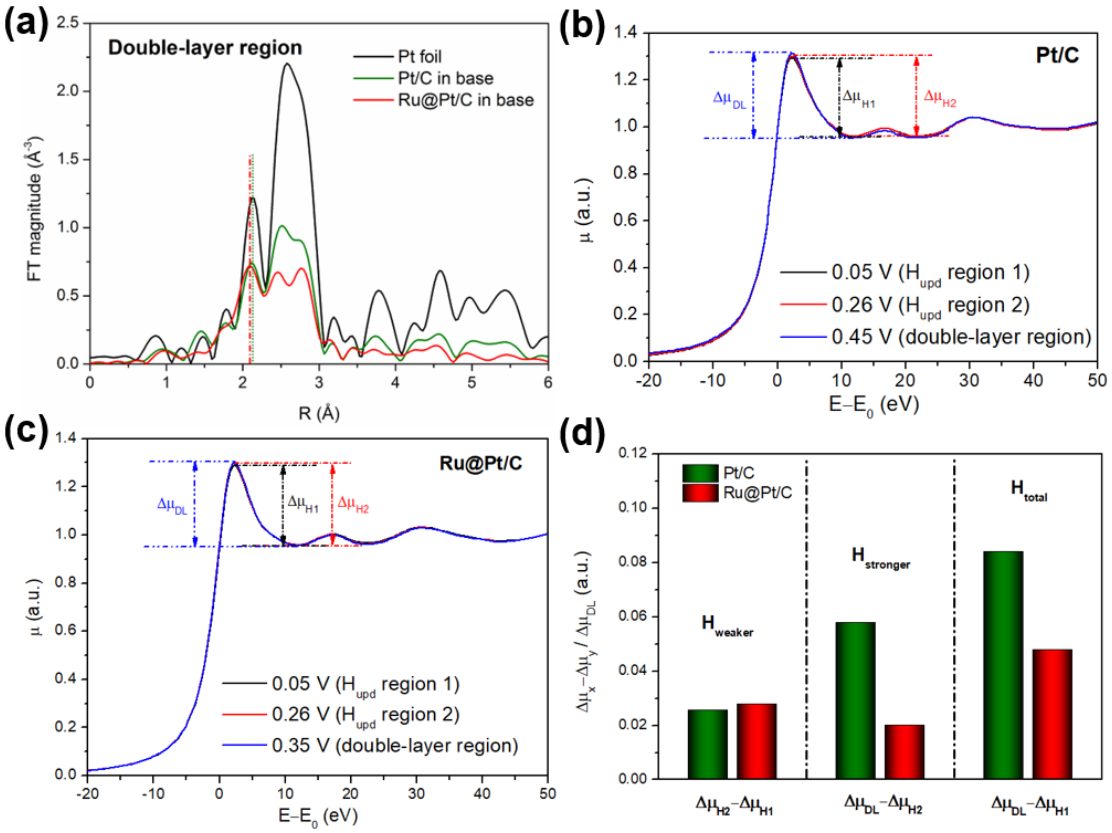

Figure 5. *In-situ* X-ray absorption studies. (a) Fourier-transform EXAFS spectra from Pt L_3 edge of Ru@Pt/C and commercial Pt/C catalysts in base at the potential of double-layer region. The potentials of double-layer region of 0.45 V *vs.* RHE for Pt/C and 0.35 V *vs.* RHE for Ru@Pt/C in base were derived from the CV curves in Figure 4a. XANES from Pt L_3 edge of (b) commercial Pt/C in 0.1 M KOH solution, and (c) Ru@Pt/C in 0.1 M KOH solution at different potentials. (d) Comparison of the relative changes in the intensity of absorption peaks for Ru@Pt/C and commercial Pt/C shown in the XANES spectra.

4. Conclusions

In summary, we have used a combination of electrochemical analysis and *in-situ* XAS analysis to address the importance of Pt—H_{ad} energetics in controlling the catalytic activity of the HOR on Pt surfaces in alkaline electrolytes. By using well-modified four

Pt surfaces with fine-tuned electronic properties, we established a clear trend in activity for HOR in base: Au@Pt < Pt < Pd@Pt < Ru@Pt, as a function of the decreasing the Pt—H_{ad} energetics. The increasing HOR activity on different Pt surfaces, as a function of the decreasing strength of the Pt—H_{ad} interaction, provides us the important way to improve the HOR kinetics. The *in-situ* XANES analysis demonstrated a higher H_{ad} coverage on the pure Pt surface than that on the Pt surface with Ru core due to more strongly bonded H_{ad} on pure Pt surface. These findings provide us a novel aspect to understand the HOR kinetics on Pt surfaces and also provides fundamental insights into the influence of the Pt—H_{ad} interaction on the HOR mechanism.

Acknowledgements

This research was performed at Brookhaven National Laboratory under contract DE-SC0012704 with the US Department of Energy, Office of Basic Energy Science, Material Science and Engineering Division, Division of Chemical Sciences, Geosciences and Biosciences Division. Beamline BL2-2 at the SSRL is supported in part by the Synchrotron Catalysis Consortium, U. S. Department of Energy Grant No DE-FG02-05ER15688. This research is also supported by Kunming University of Science and Technology (No. KKKP201707010 and KKKP201752011).

References

1. Gasteiger, H. A.; Marković, N. M., Just a Dream—or Future Reality? *Science* **2009,** *324* (5923), 48-49.

2. Dresselhaus, M. S.; Thomas, I. L., Alternative energy technologies. *Nature* **2001,** *414* (6861), 332-337.

3. Subbaraman, R.; Tripkovic, D.; Chang, K.-C.; Strmcnik, D.; Paulikas, A. P.; Hirunsit, P.; Chan, M.; Greeley, J.; Stamenkovic, V.; Markovic, N. M., Trends in activity for the water electrolyser reactions on 3d M(Ni,Co,Fe,Mn) hydr(oxy)oxide catalysts. *Nat. Mater.* **2012,** *11* (6), 550-557.

4. Strmcnik, D.; Uchimura, M.; Wang, C.; Subbaraman, R.; Danilovic, N.; van der, V.; Paulikas, A. P.; Stamenkovic, V. R.; Markovic, N. M., Improving the hydrogen oxidation reaction rate by promotion of hydroxyl adsorption. *Nat. Chem.* **2013,** *5* (4), 300-306.

5. Koper, M. T. M., Hydrogen electrocatalysis: A basic solution. *Nat. Chem.* **2013,** *5* (4), 255-256.

6. Debe, M. K., Electrocatalyst approaches and challenges for automotive fuel cells. *Nature* **2012,** *486* (7401), 43-51.

7. Gasteiger, H. A.; Kocha, S. S.; Sompalli, B.; Wagner, F. T., Activity benchmarks and requirements for Pt, Pt-alloy, and non-Pt oxygen reduction catalysts for PEMFCs. *Appl. Catal. B: Environ.* **2005,** *56* (1–2), 9-35.

8. Durst, J.; Siebel, A.; Simon, C.; Hasche, F.; Herranz, J.; Gasteiger, H. A., New insights into the electrochemical hydrogen oxidation and evolution reaction mechanism. *Energy Environ. Sci.* **2014,** *7* (7), 2255-2260.

9. Varcoe, J. R.; Slade, R. C. T., Prospects for alkaline anion-exchange membranes in low temperature fuel cells. *Fuel Cells* **2005,** *5* (2), 187-200.

10. Wang, J. X.; Springer, T. E.; Adzic, R. R., Dual-pathway kinetic equation for the hydrogen oxidation reaction on Pt electrodes. *J. Electrochem. Soc* **2006,** *153* (9),

A1732-A1740.

11. Hsieh, Y.-C.; Zhang, Y.; Su, D.; Volkov, V.; Si, R.; Wu, L.; Zhu, Y.; An, W.; Liu, P.; He, P.; Ye, S.; Adzic, R. R.; Wang, J. X., Ordered Bilayer Ruthenium–Platinum Core-Shell Nanoparticles as Carbon Monoxide-Tolerant Fuel Cell Catalysts. *Nat. Commun.* **2013,** *4*, 1-9.

12. Durst, J.; Simon, C.; Hasché, F.; Gasteiger, H. A., Hydrogen Oxidation and Evolution Reaction Kinetics on Carbon Supported Pt, Ir, Rh, and Pd Electrocatalysts in Acidic Media. *J. Electrochem. Soc* **2015,** *162* (1), F190-F203.

13. Subbaraman, R.; Tripkovic, D.; Strmcnik, D.; Chang, K.-C.; Uchimura, M.; Paulikas, A. P.; Stamenkovic, V.; Markovic, N. M., Enhancing Hydrogen Evolution Activity in Water Splitting by Tailoring Li+-Ni(OH)$_2$-Pt Interfaces. *Science* **2011,** *334* (6060), 1256-1260.

14. Danilovic, N.; Subbaraman, R.; Strmcnik, D.; Chang, K.-C.; Paulikas, A. P.; Stamenkovic, V. R.; Markovic, N. M., Enhancing the Alkaline Hydrogen Evolution Reaction Activity through the Bifunctionality of Ni(OH)2/Metal Catalysts. *Angew. Chem.* **2012,** *124* (50), 12663-12666.

15. Wang, Y.; Wang, G.; Li, G.; Huang, B.; Pan, J.; Liu, Q.; Han, J.; Xiao, L.; Lu, J.; Zhuang, L., Pt-Ru catalyzed hydrogen oxidation in alkaline media: oxophilic effect or electronic effect? *Energy Environ. Sci.* **2015,** *8* (1), 177-181.

16. Sheng, W.; Myint, M.; Chen, J. G.; Yan, Y., Correlating the hydrogen evolution reaction activity in alkaline electrolytes with the hydrogen binding energy on monometallic surfaces. *Energy Environ. Sci.* **2013,** *6* (5), 1509-1512.

17. Sheng, W.; Zhuang, Z.; Gao, M.; Zheng, J.; Chen, J. G.; Yan, Y., Correlating hydrogen oxidation and evolution activity on platinum at different pH with measured hydrogen binding energy. *Nat. Commun.* **2015,** *6*.

18. Adzic, R.; Zhang, J.; Sasaki, K.; Vukmirovic, M.; Shao, M.; Wang, J.; Nilekar, A.; Mavrikakis, M.; Valerio, J.; Uribe, F., Platinum Monolayer Fuel Cell Electrocatalysts. *Top. Catal.* **2007,** *46* (null), 249-262.

19. Hammer, B.; Nørskov, J. K., Theoretical surface science and catalysis—calculations and concepts. In *Advances in Catalysis*, Bruce C. Gates, H. K., Ed. Academic Press: 2000; Vol. Volume 45, pp 71-129.

20. Zhang, Y.; Hsieh, Y. C.; Volkov, V.; Su, D.; An, W.; Si, R.; Zhu, Y. M.; Liu, P.; Wang, J. X.; Adzic, R. R., High Performance Pt Mono layer Catalysts Produced via Core-Catalyzed Coating in Ethanol. *Acs Catal.* **2014,** *4* (3), 738-742.

21. McBreen, J.; O'Grady, W. E.; Pandya, K. I.; Hoffman, R. W.; Sayers, D. E., EXAFS study of the nickel oxide electrode. *Langmuir* **1987,** *3* (3), 428-433.

22. Sasaki, K.; Wang, J. X.; Naohara, H.; Marinkovic, N.; More, K.; Inada, H.; Adzic, R. R., Recent advances in platinum monolayer electrocatalysts for oxygen reduction reaction: Scale-up synthesis, structure and activity of Pt shells on Pd cores. *Electrochim. Acta* **2010,** *55* (8), 2645-2652.

23. Ravel, B.; Newville, M., ATHENA, ARTEMIS, HEPHAESTUS: data analysis for X-ray absorption spectroscopy using IFEFFIT. *J. Synchrotron Rad.* **2005,** *12* (4), 537-541.

24. Rheinländer, P. J.; Herranz, J.; Durst, J.; Gasteiger, H. A., Kinetics of the Hydrogen

Oxidation/Evolution Reaction on Polycrystalline Platinum in Alkaline Electrolyte Reaction Order with Respect to Hydrogen Pressure. *J. Electrochem. Soc* **2014,** *161* (14), F1448-F1457.

25. Sheng, W.; Gasteiger, H. A.; Shao-Horn, Y., Hydrogen Oxidation and Evolution Reaction Kinetics on Platinum: Acid vs Alkaline Electrolytes. *J. Electrochem. Soc* **2010,** *157* (11), B1529-B1536.

26. StrmcnikD; KodamaK; van der Vliet, D.; GreeleyJ; Stamenkovic, V. R.; Marković, N. M., The role of non-covalent interactions in electrocatalytic fuel-cell reactions on platinum. *Nat. Chem.* **2009,** *1* (6), 466-472.

27. Schouten, K. J. P.; van der Niet, M. J. T. C.; Koper, M. T. M., Impedance spectroscopy of H and OH adsorption on stepped single-crystal platinum electrodes in alkaline and acidic media. *Phys. Chem. Chem. Phys* **2010,** *12* (46), 15217-15224.

28. Sie, S. T.; Maxwell, J. E.; Minderhoud, J. K.; Stork, W. J. H.; van Veen, J. A. R.; Weitkamp, J.; Traa, Y.; O'Connor, C. T.; Heinemann, H.; Whitehurst, D. D.; Gorbaty, M. L.; Vielstich, W.; Iwasita, T.; Pichat, P., Energy-related catalysis: sections 3.12.5 – 3.19.8. In *Handbook of Heterogeneous Catalysis*, Wiley-VCH Verlag GmbH: 2008; pp 2006-2122.

29. van der Vliet, D. F.; Wang, C.; Li, D.; Paulikas, A. P.; Greeley, J.; Rankin, R. B.; Strmcnik, D.; Tripkovic, D.; Markovic, N. M.; Stamenkovic, V. R., Unique Electrochemical Adsorption Properties of Pt-Skin Surfaces. *Angew. Chem. Int. Ed.* **2012,** *124* (13), 3193-3196.

30. Conway, B. E.; Tilak, B. V., Interfacial processes involving electrocatalytic

evolution and oxidation of H2, and the role of chemisorbed H. *Electrochim. Acta* **2002,** *47* (22–23), 3571-3594.

31. Marković, N. M.; Grgur, B. N.; Ross, P. N., Temperature-Dependent Hydrogen Electrochemistry on Platinum Low-Index Single-Crystal Surfaces in Acid Solutions. *J. Phys. Chem. B* **1997,** *101* (27), 5405-5413.

32. Gasteiger, H. A.; Markovic, N. M.; Ross, P. N., H2 and CO Electrooxidation on Well-Characterized Pt, Ru, and Pt-Ru. 1. Rotating Disk Electrode Studies of the Pure Gases Including Temperature Effects. *J. Phys. Chem.* **1995,** *99* (20), 8290-8301.

33. Krischer, K.; Savinova, E. R., *Handbook of Heterogeneous Catalysis*. Wiley-VCH: Chichhester, 2009; p 1873-1905.

34. Xu, Y.; Ruban, A. V.; Mavrikakis, M., Adsorption and Dissociation of O2 on Pt−Co and Pt−Fe Alloys. *J. Am. Chem. Soc.* **2004,** *126* (14), 4717-4725.

35. Chen, W.-F.; Sasaki, K.; Ma, C.; Frenkel, A. I.; Marinkovic, N.; Muckerman, J. T.; Zhu, Y.; Adzic, R. R., Hydrogen-Evolution Catalysts Based on Non-Noble Metal Nickel–Molybdenum Nitride Nanosheets. *Angew. Chem. Int. Ed.* **2012,** *51* (25), 6131-6135.

36. Karlberg, G. S.; Jaramillo, T. F.; Skúlason, E.; Rossmeisl, J.; Bligaard, T.; Nørskov, J. K., Cyclic Voltammograms for H on Pt(111) and Pt(100) from First Principles. *Phys. Rev. Lett.* **2007,** *99* (12), 126101.

37. GreeleyJ; Stephens, I. E. L.; Bondarenko, A. S.; Johansson, T. P.; Hansen, H. A.; Jaramillo, T. F.; RossmeislJ; ChorkendorffI; Nørskov, J. K., Alloys of platinum and early transition metals as oxygen reduction electrocatalysts. *Nat. Chem.* **2009,** *1* (7),

552-556.

38. Joo, S. H.; Choi, S. J.; Oh, I.; Kwak, J.; Liu, Z.; Terasaki, O.; Ryoo, R., Ordered nanoporous arrays of carbon supporting high dispersions of platinum nanoparticles. *Nature* **2001,** *412* (6843), 169-172.

39. Sasaki, K.; Zhang, J.; Wang, J.; Uribe, F.; Adzic, R., Platinum submonolayer–monolayer electrocatalysts: an electrochemical and X-ray absorption spectroscopy study. *Research on Chemical Intermediates* **2006,** *32* (5), 543-559.